

# On the collisional damping of plasma velocity space instabilities

Yanzeng Zhang and Xian-Zhu Tang

Theoretical Division, Los Alamos National Laboratory, Los Alamos, New Mexico 87545, USA

For plasma velocity space instabilities driven by particle distributions significantly deviated from a Maxwellian, weak collisions can damp the instabilities by an amount that is significantly beyond the collisional rate itself. This is attributed to the dual role of collisions that tend to relax the plasma distribution toward a Maxwellian and to suppress the linearly perturbed distribution function. The former effect can dominate in cases where the unstable non-Maxwellian distribution is driven by collisionless transport on a time scale much shorter than that of collisions, and the growth rate of the ideal instability has a sensitive dependence on the distribution function. The whistler instability driven by electrostatically trapped electrons is used as an example to elucidate such a strong collisional damping effect of plasma velocity space instabilities, which is confirmed by first-principles kinetic simulations.

Plasmas of astrophysical, space and laboratory origins are known to support a wide variety of waves and instabilities<sup>1-6</sup>. These waves and instabilities are of great importance for plasma transport, heating, confinement, and diagnostics. A large family of plasma instabilities falls under the category of ideal modes, as they are excited in the absence of collisions that would introduce dissipation into an otherwise Hamiltonian system. Plasma collisions typically reduce the growth rate of these ideal modes, also known by the term collisional damping in plasma physics. This can be contrasted with the family of the so-called resistive or dissipative modes that rely on collisions to destabilize an otherwise stable or marginal ideal mode. Well-known examples of such include the resistive tearing modes<sup>7</sup> and a class of dissipative drift wave instabilities<sup>8</sup>. Here we focus on the collisional damping of ideal modes.

The common expectation is that the collisional damping rate,  $\Gamma_v = \gamma_0 - \gamma$  with  $\gamma_0$  and  $\gamma$  the growth rates without and with collisions, respectively, is approximately the collisional rate<sup>9-14</sup>, which for electrons is  $\nu = 4\sqrt{2}\pi n_e e^4 \ln\Lambda / (3m_e^{1/2} T_e^{3/2})$  with  $\ln\Lambda$  the Coulomb logarithm. This can be understood by considering the Boltzmann equation

$$\frac{df}{dt} = \frac{\partial f}{\partial t} + \mathbf{v} \cdot \nabla f + \frac{q}{m} \left( \mathbf{E} + \frac{\mathbf{v} \times \mathbf{B}}{c} \right) \cdot \nabla_{\mathbf{v}} f = C(f), \quad (1)$$

where  $C(f)$  is the collision operator. The stability analysis starts with identifying an equilibrium distribution  $f_0$ , along with the equilibrium electromagnetic field  $(\mathbf{E}_0, \mathbf{B}_0)$ , that satisfies

$$\mathbf{v} \cdot \nabla f_0 + \frac{q}{m} \left( \mathbf{E}_0 + \frac{\mathbf{v} \times \mathbf{B}_0}{c} \right) \cdot \nabla_{\mathbf{v}} f_0 = C(f_0), \quad (2)$$

The perturbed distribution  $f_1$  and the perturbed electromagnetic field  $(\mathbf{E}_1, \mathbf{B}_1)$ , to linear order, follow,

$$\begin{aligned} \frac{\partial f_1}{\partial t} + \mathbf{v} \cdot \nabla f_1 + \frac{q}{m} \left( \mathbf{E}_0 + \frac{\mathbf{v} \times \mathbf{B}_0}{c} \right) \cdot \nabla_{\mathbf{v}} f_1 \\ + \frac{q}{m} \left( \mathbf{E}_1 + \frac{\mathbf{v} \times \mathbf{B}_1}{c} \right) \cdot \nabla_{\mathbf{v}} f_0 = C(f_0 + f_1) - C(f_0). \end{aligned} \quad (3)$$

The collisional damping of a linearly unstable mode  $(f_1, \mathbf{E}_1, \mathbf{B}_1)$  can be understood by considering a Krook-like

approximation of the collision operator<sup>15</sup>,

$$C(f) = -\nu(f - f_M), \quad (4)$$

which signifies the fact that collisions will relax the particle distribution function  $f$  to a Maxwellian  $f_M$  over a time period of  $\nu^{-1}$ . This leads to  $C(f_0 + f_1) - C(f_0) \approx -\nu f_1$  in Eq. (3), which means that collisions will only affect the linearly perturbed distribution  $f_1$ , the effect of which can be absorbed into the temporal derivative in Eq. (3), without changing other terms, as

$$\frac{\partial f_1}{\partial t} + \nu f_1 = -i(\omega + i\nu)f_1, \quad (5)$$

where  $\omega$  is the mode/wave frequency. The physics implication of Eq. (5) is that the collisions will cause damping of the waves/instabilities by the amount of  $\Gamma_v = \nu$ . It is important to note that such absorption of  $\nu$  into  $\omega$  is not applicable to Maxwell's equations. In the fluid picture, this means that the substitution  $\omega \rightarrow \omega + i\nu$  is only permissible in the conductivity tensor but not the entire wave dispersion relation<sup>14</sup>. However, as one can imagine, even such part substitution would lead to a damping rate  $\Gamma_v \sim \nu$ , reinforcing the conventional wisdom that the collisional damping can be important only when  $\nu \sim \gamma_0$ .

Keeping the  $C(f_0)$  term in Eq. (2) implies that the unstable equilibrium distribution  $f_0$  is developed over collisional time scale. This assumption is usually not satisfied for ideal modes in which a *non-Maxwellian*  $f_0$  is formed and sustained by collisionless transport on a time scale much shorter than  $1/\nu$ , for which case  $C(f_0)$  is absent in Eq. (2). Examples of such include the laboratory sheath/presheath plasmas and tokamak plasmas undergoing thermal quench that have truncated electron distribution because of free-streaming losses<sup>16-18</sup>, and coronal and solar wind plasmas that have strongly anisotropic temperatures, non-Maxwellian tails, and energetic beam components<sup>19,20</sup>. For such unstable collisionless equilibria, the (part) substitution  $\omega \rightarrow \omega + i\nu$  of Eq. (5) can no longer adequately describe the effect of collisions on the instability. This is because weak collisions with  $\nu \ll \gamma_0 \ll \omega$  will tend to modify  $f_0$  via

$$\frac{df_0}{dt} = C(f_0) = -\nu(f_0 - f_M) \quad (6)$$

over the same time period in which  $f_1$  is collisionally damped as described by Eq. (3) or Eq. (5). Consequently, the collisional modification of  $f_0$  by an amount of  $\delta f_0$  changes the linear instability drive in Eq. (3) by the amount of

$$\frac{q}{m} \left( \mathbf{E}_1 + \frac{\mathbf{v} \times \mathbf{B}_1}{c} \right) \cdot \nabla_{\mathbf{v}} \delta f_0$$

on the left-hand side. In cases where the linear instability has a sensitive dependence on  $\delta f_0$ , which itself grows linearly in time from Eq. (6), the ideal mode can be collisionally damped mainly via this indirect channel of collisionally modified  $f_0$ . For a specific example, temperature anisotropy can drive a number of instabilities including the whistler<sup>21,22</sup>, mirror<sup>23,24</sup> and firehose<sup>25</sup> instabilities in a magnetized plasma, and Weibel instability<sup>26,27</sup> in an unmagnetized plasma. For these plasma velocity space instabilities, the modification of  $f_0$  toward  $f_M$  by weak collisions can induce further damping by weakening the drivers (e.g., the temperature anisotropy) in the velocity space. What is remarkable is that the resulting *collisional damping rate via this indirect route can be much higher than  $\Gamma_v \sim v$*  predicted by the conventional theory that does not take into account  $\delta f_0$ .

Having outlined the simple physical picture of such an enhanced collisional damping mechanism for plasma velocity space instabilities, we note that its experimental realizability requires two conditions. The first is that the unstable non-Maxwellian distribution must be developed on a time scale ( $\tau_{trans}$ ) much faster than that of the weak collisions ( $\tau_c = 1/\nu$ ). This is required to drop the  $C(f_0)$  term in Eq. (2), as noted earlier. Indeed, for a wide class of problems in the laboratory and space/astrophysics, the non-Maxwellian distribution is primarily driven by collisionless transport. A well-known laboratory example is the open field line plasma in which free-streaming loss on the time scale of  $L/v_t$  sets up a truncated Maxwellian distribution for the electrons. Here  $L$  is the length of the open field line and  $v_t = \sqrt{2T_e/m_e}$  is the electron thermal speed defined by the electron temperature  $T_e$  and electron mass  $m_e$ . If  $L$  is much shorter than the electron mean-free-path  $\lambda_{mfp}$ , the first condition would be well satisfied. In the case of solar wind where a range of velocity space instability is known to exist, the plasma collisionality is tiny and the non-Maxwellian distribution can be entirely driven by collisionless transport, for example, as a plasma adiabatic response to magnetic flux expansion that develops a highly anisotropic distribution function. We notice there are places where the solar wind can be sufficiently isotropic to stay below the temperature-anisotropy-driven instability threshold<sup>28,29</sup>, which could result from the collective effect of weak collisions.

The second condition is that the growth rate of the ideal instability has a sensitive dependence on the non-Maxwellian distribution. This is a necessity for a large impact by the collisional modification of  $f_0$  that is originally formed by collisionless transport on a time scale much shorter than that of weak collisions. In other words, since weak collisions can only modestly modify  $f_0$  on the dynamical time scale of the ideal instability, the growth rate of the ideal instability must vary significantly with a small change in  $f_0$  to observe a large

effect. Here the dynamical time scale ( $\tau_{inst}$ ) of the instability is tied to the linear growth period of the mode, so it scales inversely with the linear mode growth rate  $\gamma_0$  itself and also logarithmically with how small the initial perturbation amplitude ( $f_1^i$ ) is,

$$\tau_{inst} \approx \frac{1}{\gamma_0} \ln \frac{f_1^s}{f_1^i}. \quad (7)$$

with  $f_1^s$  the perturbation amplitude at the onset of nonlinear saturation. The first and second conditions combine to imply that in cases  $\tau_{inst}$  is not long compared with  $\tau_{trans}$ , the  $C(f_0)$  term in Eq. (2), despite its small amplitude, can already impact the linear mode at its onset due to latter's sensitivity to the details of  $f_0$ .

To illustrate the underlying physics, we employ the whistler instability, which is a common velocity space instability in the magnetized plasmas, with the temperature-anisotropy-driven one dated back many decades in space and astrophysics plasmas. Particularly, we focus on the electrostatically trapped electron driven whistler instability<sup>17</sup>, which applies to any magnetized plasma that intercepts a solid wall<sup>30-32</sup>. Notice that we focus on the linear instability and leave the nonlinear saturation physics to future works. One remarkable property of such whistler instability is that it has an instability threshold far lower than that of the whistler instability driven by the temperature anisotropy<sup>17</sup>. This was found to be critical for maintaining ambipolar transport in a steady plasma (pre)sheath<sup>17</sup> and for cooling the perpendicular electron temperature in a plasma thermal quench. It is of interest to note that the thermal quench problem is an ideal motivation for such an investigation of collisional damping of whistler instability in that the cooling of the plasma will inevitably bring the plasma from the initial collisionless regime to the eventual collisional regime<sup>33</sup>. We will show that a weak collision  $\nu \ll \gamma_0$  tends to smear the trapped-passing boundary in the parallel electron distribution function, the small modification of which can greatly reduce or even completely suppress the whistler instability. It must be emphasized that, although only the trapped electron driven whistler instability is reported here, other velocity space instabilities like the whistler and Weibel instabilities driven by the temperature anisotropy have also been investigated, and the results are in agreement with the conclusion in this paper.

Before presenting the first-principles kinetic simulations using VPIC<sup>34</sup>, we first employ a simple model to elucidate that strong damping can be achieved by slightly modifying the distribution function  $f_0$  due to the weak collisions. In the absence of collisions, the electrostatically trapped electrons can be described by a cutoff Maxwellian distribution function<sup>17</sup>

$$f_i(v_{\parallel}, v_{\perp}) = \frac{2n_e}{\text{Erf}(v_c/v_t) \sqrt{\pi} v_t^3} e^{-(v_{\parallel}^2 + v_{\perp}^2)/v_t^2} \Theta(1 - v_{\parallel}^2/v_c^2). \quad (8)$$

where  $\int_{-\infty}^{\infty} \int_0^{\infty} f_i v_{\perp} dv_{\perp} dv_{\parallel} = n_e$  for normalization. Here  $v_c \equiv \sqrt{2e|\phi_{RF}|/m_e}$  is the trapped-passing boundary in  $v_{\parallel}$ , which also affects the height of  $f_i(0,0)$  via the error function  $\text{Erf}(v_c/v_t)$ ,  $\phi_{RF}$  is the reflecting potential, and  $\Theta(x)$  is

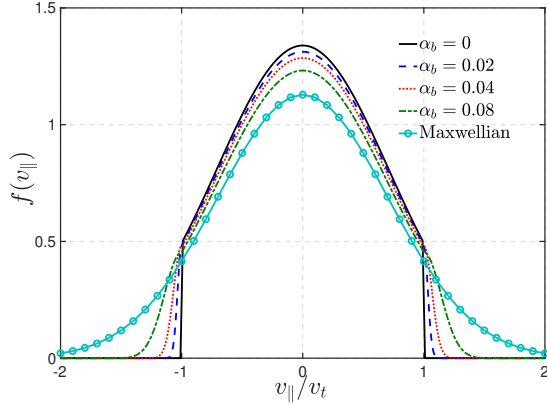


FIG. 1: Schematic view of  $f_e(v_{\parallel})$  for  $v_c = v_t$ . The Maxwellian distribution function with the same density and thermal velocity  $v_t$  is shown.

the Heaviside function. A weak collision with  $v \ll \gamma_0$  can affect the whistler instability through a smeared trapped-passing boundary, as the result of trapped electrons being scattered into the passing zone through  $C(f_0)$ . To see how such smearing of the trapped-passing boundary will greatly damp the instability, we model  $\delta f_0$ , due to weak collisions, with flow-shifted and depleted Maxwellians, which we call electron beams for convenience,

$$f_b^{\pm}(v_{\parallel}, v_{\perp}) = \frac{4n_e}{\sqrt{\pi}v_t^2 v_{tb}} e^{-v_{\perp}^2/v_t^2} e^{-(v_{\parallel} \pm v_c)^2/v_{tb}^2} \Theta[-(1 \pm v_{\parallel}/v_c)], \quad (9)$$

where  $\int_{-\infty}^{\infty} \int_0^{\infty} f_b^{\pm} v_{\perp} dv_{\perp} dv_{\parallel} = n_e$ , and  $v_{tb}$  denotes the width of  $f_b^{\pm}$  in  $v_{\parallel}$  and hence the degree of smoothness of the total distribution. Notice that such choice of  $f_b^{\pm}$  enables us to take advantage of the incomplete plasma dispersion function induced by a depleted Maxwellian<sup>35,36</sup>. As a result, the trapped electron distribution function after the smearing of trapped-passing boundary by the collisions can be modeled as

$$f_e = (1 - \alpha_b)f_t + \alpha_b(f_b^+ + f_b^-)/2, \quad (10)$$

where  $\alpha_b$  is the fraction of beam electron density. For a smooth transition of  $f_e$  at  $\pm v_c$ , we will take  $(1 - \alpha_b)f_t = \alpha_b f_b^{\pm}/2$  at  $v_{\parallel} = \pm v_c$  by using the proper  $v_{tb} = \alpha_b v_t \text{Erf}(v_c/v_t) \exp(v_c^2/v_t^2)/(1 - \alpha_b)$ . This illustrates that the larger fraction of electron beams  $\alpha_b$  will cause a smoother trapped-passing boundary (larger  $v_{tb}$ ). As an example,  $f_e$  for different  $\alpha_b$  (and thus  $v_{tb}$ ) at  $v_c = v_t$  are shown in Fig. 1.

The distribution function  $f_e$  in Eq. (10) should be placed in the dispersion relation of a whistler wave propagating along a uniform background magnetic field<sup>37</sup> with normal mode  $\text{ansatz} \exp(ikx_{\parallel} - i\omega t)$ ,

$$1 - \frac{k^2 c^2}{\omega^2} + \frac{\omega_{pe}^2}{n_e \omega} \int_{-\infty}^{\infty} \int_0^{\infty} \left[ \left(1 - \frac{kv_{\parallel}}{\omega}\right) \frac{\partial f_e}{\partial v_{\perp}^2} + \frac{kv_{\parallel}}{\omega} \frac{\partial f_e}{\partial v_{\parallel}^2} \right] \frac{v_{\perp}^3}{\omega - kv_{\parallel} - \omega_{ce}} dv_{\perp} dv_{\parallel} = 0, \quad (11)$$

where we have ignored the effect of ions assuming  $\omega_{ci} \ll \omega < \omega_{ce}$ ,  $\omega_{pe}$  is the plasma frequency,  $\omega_{ce,i}$  is the electron (ion) gyro-frequency, and  $c$  is the speed of light in a vacuum. As a result, the dispersion relation is given by

$$D(\omega, k) = 1 - \frac{k^2 c^2}{\omega^2} + (1 - \alpha_b)D_t + \alpha_b D_b = 0, \quad (12)$$

where  $D_t$  and  $D_b$  are from the trapped and beam electrons, respectively

$$D_t = \frac{\omega_{pe}^2}{\text{Erf}(\hat{v}_c) \sqrt{\pi} \omega^2} \left[ \frac{\omega}{kv_t} \int_{-\hat{v}_c}^{\hat{v}_c} \frac{e^{-\hat{v}_{\parallel}^2}}{\hat{v}_{\parallel} - \xi} d\hat{v}_{\parallel} + \frac{\hat{v}_c e^{-\hat{v}_c^2}}{\hat{v}_c^2 - \xi^2} \right], \quad (13)$$

$$D_b = \frac{\omega_{pe}^2}{\omega^2} \left[ -1 + \frac{1}{\hat{v}_{tb}^2} - \frac{1}{\sqrt{\pi}} \frac{\hat{v}_c/\hat{v}_{tb}}{\hat{v}_c^2 - \xi^2} + \sum_{\pm} \pm \frac{\hat{\omega}_{ce} + (\xi \pm \hat{v}_c)/\hat{v}_{tb}^2}{\sqrt{\pi} \hat{v}_{tb}} \int_{\mp\infty}^0 \frac{e^{-\eta^2}}{\eta - (\xi \pm \hat{v}_c)/\hat{v}_{tb}} d\eta \right], \quad (14)$$

$\hat{v}_{\parallel, c, tb} = v_{\parallel, c, tb}/v_t$ ,  $\hat{\omega}_{ce} = \omega_{ce}/kv_t$ ,  $\xi = (\omega - \omega_{ce})/kv_t$  and  $\eta = (v_{\parallel} \pm v_c)/v_{tb}$ . The integrals in Eqs. (13, 14) can be evaluated using the incomplete plasma dispersion function<sup>35,36</sup>,  $Z(w, u)$ , which is similar to the plasma dispersion function<sup>38</sup>,  $Z(w)$ , but has a cutoff at the lower limit of the integral,  $u$ .

In the absence of  $f_b^{\pm}$ , the most unstable mode (or resonant condition) satisfies  $\omega_r - \omega_{ce} \approx \pm kv_c$  (i.e.,  $\xi_r \approx \pm \hat{v}_c$ ) for whistler waves with  $\omega_r < \omega_{ce}$  as seen from  $D_t$  since there is no counterpart with  $|v_{\parallel}| > v_c$  in  $f_t$ . This means that the resonant electrons have parallel velocity  $v_{\parallel} \approx \pm v_c$  for whistler modes with  $\mp k > 0$ . However, to avoid damping in the integral induced by the singular pole along Landau-like contour, this mode will have  $|\xi|_r$  slightly greater than  $\hat{v}_c$ .

When there is a smoother boundary with  $f_e(|v_{\parallel}| > v_c) > 0$ , the resonant condition can be modified, leading to a reduction of the growth rate. Many physical insights into the impact of a smoother trapped-passing boundary on whistler instability can be obtained from the analytical solution of Eq. (12) in two limiting cases. The first one is a small cutoff speed,  $v_c \ll v_t$ . Notice that  $\omega_r - \omega_{ce} \approx kv_c \ll kv_t$  provides  $\omega_r \approx \omega_{ce}$ . Under such a condition, both  $\xi + \hat{v}_c$  and  $\xi - \hat{v}_c$  can contribute equally to  $D$  when  $\xi \approx i\gamma/(kv_t) > \hat{v}_c$ . Moreover, since  $v_{tb} \sim \alpha_b v_c/(1 - \alpha_b) \ll v_c$  for small  $\alpha_b$ , the sum of the integrals in  $D_b$  are approximated to the plasma dispersion function with a large argument. As a result, if  $|\omega/(kv_t)| \ll |1/\xi|$ , one finds in the limit of  $k^2 c^2 \gg \omega^2$  that

$$D = -\frac{k^2 c^2}{\omega^2} + (1 - \alpha_b) \frac{\omega_{pe}^2}{2\omega^2} \frac{k^2 v_t^2}{\gamma^2} + \alpha_b \frac{\omega_{pe}^2}{2\omega^2} \frac{k^2 v_t^2}{\gamma^2}, \quad (15)$$

where the second (third) term is from the trapped electrons (electron beams), and the approximation of  $\text{Erf}(x) \rightarrow 1.125x$  is invoked for  $x \ll 1$ . Eq. (15) illustrates that the electron beams do not affect the whistler instability for  $v_c \ll v_t$ , yielding a solution  $\omega \approx \omega_{ce} + i\omega_{pe} v_t/\sqrt{2}c$ . This is not surprising considering that a delta-function-like profile of  $f_b^{\pm}$  at  $v_{tb} \ll v_c \ll v_t$  does not introduce appreciable smoothing.

For a general cutoff velocity,  $v_c \sim v_t$ , we can consider a small fraction of electron beams  $\alpha_b \ll 1$  (weak smoothing) so that  $\hat{v}_{tb} \ll |\xi \pm \hat{v}_c|$ . Notice that for the most unstable mode with  $k > 0$  ( $k < 0$ ), there is only one resonant condition  $\xi = -\hat{v}_c$  ( $\xi = \hat{v}_c$ ). As a result, the incomplete plasma dispersion functions in  $D_b$  can be approximated by an asymptotic expansion of the large argument to find,

$$D_b \approx \frac{\omega_{pe}^2}{\omega^2} \left[ -1 + \frac{\hat{\omega}_{ce}\xi}{\hat{v}_c^2 - \xi^2} - \frac{1}{2} \frac{\xi^2 + \hat{v}_c^2}{(\xi^2 - \hat{v}_c^2)^2} \right]. \quad (16)$$

This approximation is also applicable to the small  $v_c$  limit, where the third term in the bracket dominates for small  $\xi$ , providing the third term in Eq. (15). While  $D_t$  can be approximated as

$$D_t \approx \frac{\omega_{pe}^2}{\omega^2} \left\{ \frac{\omega_r}{kv_c} + i \left[ \frac{\omega_r}{(kv_c)^2} \gamma - \frac{kv_t e^{-\hat{v}_c^2}}{2\sqrt{\pi}\gamma} \right] \right\}. \quad (17)$$

In the limit of  $k^2 c^2 \gg \omega^2$ , the growth rate is given by  $(1 - \alpha_b)Im(D_t) + \alpha_b Im(D_b) = 0$ , where the factor  $\omega_{pe}^2/\omega^2$  has been excluded from  $D$ . This yields

$$(1 - \alpha_b) \left[ \frac{\omega_r}{(kv_c)^2} \gamma - \frac{kv_t e^{-\hat{v}_c^2}}{2\sqrt{\pi}\gamma} \right] + \alpha_b \frac{\omega_{ce}}{2\gamma} = 0, \quad (18)$$

where the resonant condition is assumed to be exactly  $|\xi_r| = \hat{v}_c$  and thus the third term in Eq. (16) can be ignored for the imaginary part. Eq. (18) indicates that the electron beams will reduce the whistler instability and even completely suppress it when  $\alpha_b \gtrsim \alpha_b^{th} \equiv kv_t \exp(-\hat{v}_c^2)/(\sqrt{\pi}\omega_{ce})$ .

For a thermal quench problem, the numerical solutions of Eq. (12) are plotted in Fig. 2 for the real frequency and growth rate of the most unstable mode. It shows that for  $v_c \sim v_t$ , the growth rate is greatly reduced by a smoother trapped-passing boundary. Such a reduction is more significant for larger  $v_c$  and  $\alpha_b$  as suggested by Eq. (18). For sufficiently large  $\alpha_b$ , which depends on  $v_c$ , the instability can be completely suppressed. In contrast, for small  $v_c \ll v_t$ , the damping effect is small (and negligible for  $v_c \lesssim 0.1v_t$  from numerical solutions that are not shown), in good agreement with Eq. (15).

Fig. 2 demonstrates that the smearing of the trapped-passing boundary will also reduce the real frequency and hence the wavenumber of the whistler mode. This is because the resonant condition  $\omega - kv_{\parallel} = \omega_{ce}$  will cover larger  $v_{\parallel} > v_c$  and hence smaller  $\omega$  and  $k$  with smoother trapped-passing boundary. Such property indicates that the damping of velocity space instabilities due to  $C(f_0)$  is realized through changing the resonant condition due to the modification of the distribution function  $f_0$ .

Although such model analysis confirms that moderate smearing of the trapped-passing boundary, which is physically due to weak collisions where  $\alpha_b$  increases with the collisional rate  $\nu$ , can cause appreciable damping ( $\Gamma_{\nu} = \gamma_0 - \gamma \sim \gamma_0$ ) of the whistler instability, the quantification of  $\Gamma_{\nu}$  with  $\nu$  can only be obtained by deploying the first-principles kinetic simulations. Here we employ 1D3V PIC simulations using the VPIC code<sup>34</sup>, which is relativistic, to investigate the whistler instability driven by the trapped electrons. A uniform plasma

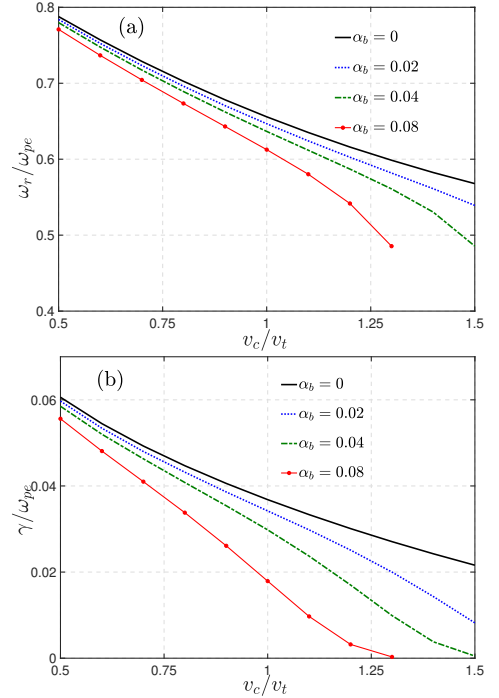


FIG. 2: Real frequency (a) and growth rate (b) of the most unstable mode for different  $\alpha_b$  corresponding to figure 1. The plasma parameters are chosen from a thermal quench problem of a fusion-grade plasma with density  $n_e = 10^{19} m^{-3}$ , temperature  $T_e = T_i = 10keV$ , and an external magnetic field,  $B_0$  so that  $\beta_e \equiv 8\pi n_e T_e / B_0^2 = 4\%$ .

with parameters corresponding to Fig. 2 is initiated in a periodic box with a length of  $L_x = 1400\lambda_D$  with  $\lambda_D$  being the Debye length. The ion distribution function is a Maxwellian but electrons are drawn from  $f_i$  in Eq. (8). Reduced ion mass  $m_i = 100m_e$  is used. The resolution of the simulation is  $\Delta x = 0.1\lambda_D$  with 5000 macro-particles per cell. Takizuka and Abe's method<sup>39</sup> is employed as the collisional model in VPIC, where we vary the collisional rate by utilizing an artificial Coulomb logarithm  $\ln\Lambda$ . Notice that the most unstable mode will arise from the incoherent thermal noise in VPIC and become dominant over time. The key idea for such simulations is that even weak collisions  $\nu \ll \gamma_0 \sim 10^{-2}\omega_{pe}$  can cause smearing of the trapped-passing boundary in the time period of  $\gamma_0^{-1}$  so that the linear growth rate will decrease with time compared to that for the collisionless case.

In Fig. 3, we show the time evolution of the amplitude of the perturbed transverse magnetic field for the most unstable mode with an initial cutoff velocity of  $v_c = v_t$ . In the absence of collisions, the electron distribution function in the linear regime remains a cutoff Maxwellian (e.g., see Fig. 4). As a result, the growth rate remains nearly constant (e.g., see Fig. 3), which is fitted as  $\gamma_0 = 0.029\omega_{pe}$ . We notice that such a growth rate is smaller than the analytical result in Fig. 2 with  $\alpha = 0$ , where  $\gamma_0 = 0.036\omega_{pe}$ . This is because the distribution in VPIC cannot sustain a cutoff Maxwellian with a discontinuity, so the trapped-passing boundary will be slightly smoothed as shown

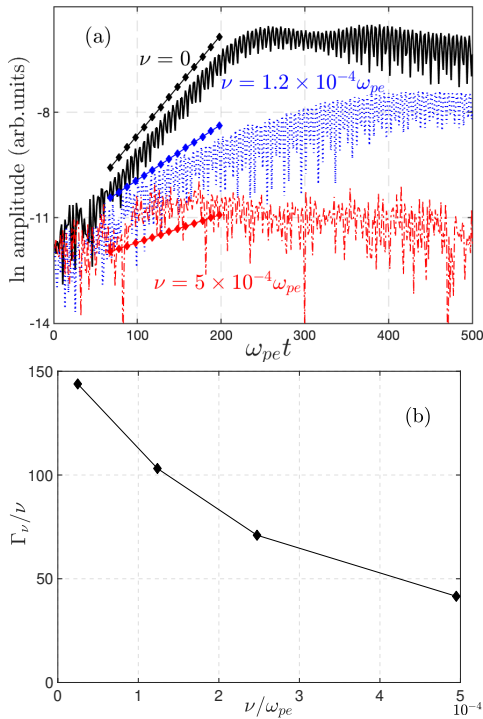


FIG. 3: (a) Time evolution of the amplitude of perturbed magnetic field (in natural-log scale) for the most unstable mode (the solid lines labeled by diamonds illustrate the fitted slope). and (b) the collisional damping rate versus the collisional rate for  $v_c = v_t$ .

in Fig. 4 starting from the first-step advancement of the simulations. As a result, the growth rate should be smaller than that of an exact cutoff Maxwellian, reinforcing the observation that the linear growth rate has a sensitive dependence on the fine details of the distribution function. In fact, if we integrate the numerical distribution from VPIC to the dispersion relation in Eq. (11), we obtain  $\gamma_0 = 0.03\omega_{pe}$ , agreeing well with the fitted growth rate from Fig. 3.

Fig. 3 shows that even weak collisions  $\nu \ll \gamma_0$  will continuously smear the trapped-passing boundary (e.g., see Fig. 4), which, according to our model analysis, will cause increasing damping of the linear instability with time. For such cases, there are two regimes concerning the collisional rate: (1) if the collision is so weak that the modification of  $f_t$  before nonlinear saturation is moderate, the whistler modes keep growing with decreasing growth rate; and (2) if the collisional rate is relatively large, the smearing of the trapped-passing boundary will reach the point that all unstable modes are suppressed. These two regimes have been illustrated in Fig. 3(a), where the transition of them occurs at  $\nu \sim 10^{-4}\omega_{pe} \ll \gamma_0$ .

The growth rates of whistler instability with collisions are fitted by avoiding the early time  $\omega_{pet} > 100$  to illustrate the strong collisional damping effect as shown in Fig. 3(a), from which we have plotted  $\Gamma_\nu/\nu$  versus  $\nu$  in Fig. 3(b). A remarkable finding is that  $\Gamma_\nu$  is two orders of magnitude larger than  $\nu$ , which is much stronger than the conventional theory of collisional damping rate with  $\Gamma_\nu/\nu \sim 1$ . It is interesting to note

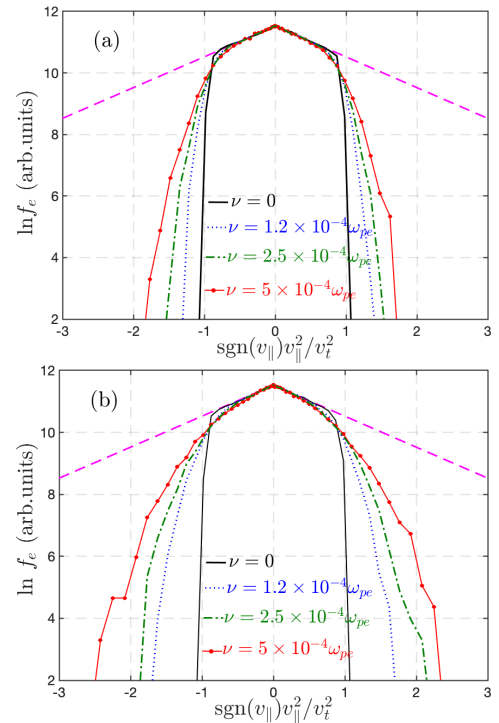


FIG. 4: Parallel electron distribution functions at  $\omega_{pet} \approx 41$  and (b)  $\omega_{pet} \approx 150$  for different  $\nu$  corresponding Fig. 3. The dashed line (magenta) represents the Maxwellian distribution function.

that  $\gamma \sim 10^{-2}\omega_{pe}$  for the whistler instability and thus appreciable collisional damping of the whistler instability requires  $\nu \sim 10^{-4}\omega_{pe}$ . In such a regime, the condition that  $f_0$  is determined by the hot tail electron loss mechanism instead of collisions, i.e.,  $\tau_{trans} \sim L/v_c \ll \tau_c \sim 1/\nu$ , requiring  $L/v_c \sim 10^3\omega_{pe}^{-1}$  or  $L \sim 10^3\lambda_D$ , which can be satisfied in magnetized plasmas that intercept a solid wall.

In conclusion, we have shown that a drastically enhanced collisional damping is realized for the ideal mode driven by an equilibrium  $f_0$  reached in the collisionless limit that is significantly deviated from a Maxwellian. Such stronger collisional damping is due to the modification of  $f_0$  via collision operator  $C(f_0)$  as opposed to the damping of  $f_1$  via  $C(f_1)$ . An example of the trapped electron driven whistler instability is used to elucidate such a mechanism, where weak collisions can cause a significant damping of the instability by smearing the trapped-passing boundary. The first-principles simulations show that  $\Gamma_\nu/\nu \sim 10^2$ , which is much beyond the conventional theory when  $\delta f_0$  is not taken into account.

We thank the U.S. Department of Energy Office of Fusion Energy Sciences and Office of Advanced Scientific Computing Research for support under the Tokamak Disruption Simulation (TDS) Scientific Discovery through Advanced Computing (SciDAC) project, and the Base Theory Program, both at Los Alamos National Laboratory (LANL) under contract No. 89233218CNA000001. Y.Z. is supported under a Director's Postdoctoral Fellowship at LANL. This research used resources of the National Energy Research Scientific Comput-

ing Center (NERSC), a U.S. Department of Energy Office of Science User Facility operated under Contract No. DE-AC02-05CH11231 and the Los Alamos National Laboratory Institutional Computing Program, which is supported by the U.S. Department of Energy National Nuclear Security Administration under Contract No. 89233218CNA000001.

- <sup>1</sup>T. H. Stix, *Waves in plasmas* (Springer Science & Business Media, 1992).
- <sup>2</sup>D. G. Swanson, *Plasma waves* (CRC Press, 2003).
- <sup>3</sup>I. B. Bernstein, "Waves in a plasma in a magnetic field," *Physical Review* **109**, 10 (1958).
- <sup>4</sup>B. V. Somov, "Wave-particle interaction in astrophysical plasma," in *Plasma Astrophysics, Part I* (Springer, 2013) pp. 129–146.
- <sup>5</sup>D. B. Melrose, *Instabilities in space and laboratory plasmas* (1986).
- <sup>6</sup>L. Chen, *Waves and instabilities in plasmas*, Vol. 12 (World scientific, 1987).
- <sup>7</sup>H. P. Furth, J. Killeen, and M. N. Rosenbluth, "Finite-resistivity instabilities of a sheet pinch," *The physics of Fluids* **6**, 459–484 (1963).
- <sup>8</sup>A. Hasegawa and M. Wakatani, "Plasma edge turbulence," *Physical Review Letters* **50**, 682 (1983).
- <sup>9</sup>E. Epperlein, R. Short, and A. Simon, "Damping of ion-acoustic waves in the presence of electron-ion collisions," *Physical review letters* **69**, 1765 (1992).
- <sup>10</sup>C. Ng, A. Bhattacharjee, and F. Skiff, "Kinetic eigenmodes and discrete spectrum of plasma oscillations in a weakly collisional plasma," *Physical review letters* **83**, 1974 (1999).
- <sup>11</sup>A. Lenard and I. B. Bernstein, "Plasma oscillations with diffusion in velocity space," *Physical Review* **112**, 1456 (1958).
- <sup>12</sup>S. De Souza-Machado, M. Sarfaty, and F. Skiff, "Kinetic modes in a hot magnetized and weakly collisional plasma," *Physics of Plasmas* **6**, 2323–2331 (1999).
- <sup>13</sup>M. Brambilla, "The effects of coulomb collisions on the propagation of cold-plasma waves," *Physics of Plasmas* **2**, 1094–1099 (1995).
- <sup>14</sup>P. Aleynikov and B. Breizman, "Stability analysis of runaway-driven waves in a tokamak," *Nuclear Fusion* **55**, 043014 (2015).
- <sup>15</sup>P. L. Bhatnagar, E. P. Gross, and M. Krook, "A model for collision processes in gases. i. small amplitude processes in charged and neutral one-component systems," *Physical review* **94**, 511 (1954).
- <sup>16</sup>X.-Z. Tang, "Kinetic magnetic dynamo in a sheath-limited high-temperature and low-density plasma," *Plasma Physics and Controlled Fusion* **53**, 082002 (2011).
- <sup>17</sup>Z. Guo and X.-Z. Tang, "Ambipolar transport via trapped-electron whistler instability along open magnetic field lines," *Physical review letters* **109**, 135005 (2012).
- <sup>18</sup>Y. Zhang, J. Li, and X.-Z. Tang, "Cooling flow regime of plasma thermal quench." Submitted to *Europhysics Letters*, <https://arxiv.org/abs/2207.09974> (2022).
- <sup>19</sup>E. Marsch, "Kinetic physics of the solar corona and solar wind," *Living Reviews in Solar Physics* **3**, 1 (2006).
- <sup>20</sup>M. Lazar, R. López, S. M. Shaaban, S. Poedts, P. H. Yoon, and H. Fichtner, "Temperature anisotropy instabilities stimulated by the solar wind suprathermal populations," *Frontiers in Astronomy and Space Sciences* **8** (2022), 10.3389/fspas.2021.777559.
- <sup>21</sup>C. F. Kennel and H. Petschek, "Limit on stably trapped particle fluxes," *Journal of Geophysical Research* **71**, 1–28 (1966).
- <sup>22</sup>S. P. Gary and J. Wang, "Whistler instability: Electron anisotropy upper bound," *Journal of Geophysical Research: Space Physics* **101**, 10749–10754 (1996).
- <sup>23</sup>D. J. Southwood and M. G. Kivelson, "Mirror instability: 1. physical mechanism of linear instability," *Journal of Geophysical Research: Space Physics* **98**, 9181–9187 (1993).
- <sup>24</sup>O. A. Pokhotelov, R. A. Treumann, R. Z. Sagdeev, M. A. Balikhin, O. G. Onishchenko, V. P. Pavlenko, and I. Sandberg, "Linear theory of the mirror instability in non-maxwellian space plasmas," *Journal of Geophysical Research: Space Physics* **107**, SMP-18 (2002).
- <sup>25</sup>J. V. Hollweg and H. Völk, "New plasma instabilities in the solar wind," *Journal of Geophysical Research* **75**, 5297–5309 (1970).
- <sup>26</sup>E. S. Weibel, "Spontaneously growing transverse waves in a plasma due to an anisotropic velocity distribution," *Physical Review Letters* **2**, 83 (1959).
- <sup>27</sup>G. Kalman, C. Montes, and D. Quémada, "Anisotropic temperature plasma instabilities," *The Physics of Fluids* **11**, 1797–1808 (1968).
- <sup>28</sup>D. Verscharen, K. G. Klein, and B. A. Maruca, "The multi-scale nature of the solar wind," *Living Reviews in Solar Physics* **16**, 1–136 (2019).
- <sup>29</sup>P. Yoon, J. Seough, C. Salem, and K. Klein, "Solar wind temperature isotropy," *Physical review letters* **123**, 145101 (2019).
- <sup>30</sup>V. Godyak, R. Piejak, and B. Alexandrovich, "Measurement of electron energy distribution in low-pressure rf discharges," *Plasma sources science and technology* **1**, 36 (1992).
- <sup>31</sup>P. C. Stangeby *et al.*, *The plasma boundary of magnetic fusion devices*, Vol. 224 (Institute of Physics Pub. Philadelphia, Pennsylvania, 2000).
- <sup>32</sup>L. Dorf and V. Semenov, "Energy flow through a nonambipolar langmuir sheath," *Physics of Plasmas* **16**, 073501 (2009).
- <sup>33</sup>J. Li, Y. Zhang, and X.-Z. Tang, "Staged cooling of a fusion-grade plasma in a tokamak thermal quench," Submitted to *Nuclear Fusion* (2022), <https://doi.org/10.48550/arXiv.2211.06781>.
- <sup>34</sup>K. J. Bowers, B. Albright, L. Yin, B. Bergen, and T. Kwan, "Ultrahigh performance three-dimensional electromagnetic relativistic kinetic plasma simulation," *Physics of Plasmas* **15**, 055703 (2008).
- <sup>35</sup>R. Franklin, "Proceedings of the tenth international conference on phenomena in ionized gases," (1971).
- <sup>36</sup>S. D. Baalrud, "The incomplete plasma dispersion function: Properties and application to waves in bounded plasmas," *Physics of Plasmas* **20**, 012118 (2013).
- <sup>37</sup>N. A. Krall and A. W. Trivelpiece, *Principles of plasma physics* (San Francisco Press, Inc., San Francisco, 1986).
- <sup>38</sup>B. D. Fried and S. C. Conte, *The Plasma Dispersion Function* (Academic, New York, 1961).
- <sup>39</sup>T. Takizuka and H. Abe, "A binary collision model for plasma simulation with a particle code," *Journal of Computational Physics* **25**, 205 – 219 (1977).